ORIGINAL PAPER

Rock slope stability analysis under Hoek–Brown failure criterion with different flow rules

Svetlana Melentijević[1] · Zoran Berisavljević[2] · Dusan Berisavljević[2] · Claudio Olalla Marañón[3]

Abstract

The stability analysis of homogeneous rock slope following the Hoek–Brown failure criterion under the hypothesis of different flow rules is performed based on limit equilibrium and finite element methods. The applied failure criterion is the generalized Hoek–Brown that can be introduced as a shear/normal function in analysis applying different flow rules. The results are compared with those obtained by the application of equivalent shear strength parameters of the Mohr–Coulomb criterion, considering that this is still the most widely used criterion in rock slope stability analysis and is still the base for the shear strength reduction method applied in finite element modelling. Different proposals for estimating the equivalent strength parameters based on confining stress level are evaluated. The limitation of stress-dependent linear Mohr–Coulomb parameters is emphasized by analysing the vertical cut problem, for which, depending on the chosen stress level, different critical heights are obtained for the same material. Sensitivity analysis of geotechnical parameters used as input for failure criterion is performed to determine their influence on slope stability. Probabilistic analysis is conducted to determine the probability of failure when different flow rules are applied. If slope stability analysis is performed with an assumption of associative flow rule, the probability of failure is within the acceptable limits for the considered case study, while employing non-associative flow rule, the probability of failure is rather high. The chart is presented that could be readily used to estimate the combination of σ_{ci}, GSI, and m_i values that produce failure for the analysed case study.

Keywords Circular failure surface · Hoek and Brown failure criterion · Flow rule · Shear/normal function · Stress level · Probabilistic and sensitivity analysis

Abbreviations

c'	Cohesion
m_i	Rock mass constant
m_b	Reduced value of the intact rock mass constant m_i
m_{dil}	Dilation parameter
s and a	Rock mass material constants

p, q	Lambe's variables
p*, q*	Dimensionless form of Lambe's variables
CoF	Consequence of failure
CoV	Coefficient of variation
D	Disturbance factor
E_{rm}	Deformation modulus of the rock mass
E_i	Elastic modulus of intact rock
FS	Factor of safety
GSI	Geological strength index
H	Slope height
H*	Dimensionless height
H_L	Lower bound solution for critical height of vertical cut
H_U	Upper bound solution for critical height of vertical cut
K_0	Initial value of lateral earth pressure coefficient
P_f	Probability of failure
RI	Reliability index
SD	Standard deviation of FS

✉ Svetlana Melentijević
svmelent@ucm.es

1 Department of Geodynamics, Stratigraphy and Paleonthology, Faculty of Geological Science, Universidad Complutense de Madrid, c/ José Antonio Nováis 12, Ciudad Universitaria, 28040 Madrid, Spain

2 Department of Geotechnics, Faculty of Mining and Geology, University of Belgrade, 7 Djusina Street, 11000 Belgrade, Serbia

3 Department of Geotechnics, ETSI Caminos Canales y Puertos, Universidad Politécnica de Madrid, c/ Profesor Aranguren 3, 28040 Madrid, Spain

β	Strength modulus used to scale the original HB failure criterion
β_a	Strength modulus used to scale the generalized HB failure criterion
δ	Angle of slope inclination
$\phi\prime$	Instantaneous friction angle
γ	Unit weight
$\sigma_1^{\prime}$	Major principal stresses at failure
σ_3	Minor principal stresses at failure
$\sigma\prime_{3max}$	Upper limit of the confining stress
σ_{ci}	Uniaxial compressive strength of the intact rock
$\sigma\prime_{cm}$	Rock mass compressive strength
σ_t	Tensile strength of the rock mass
τ	Tangential stress exerted on the failure surface
σ	Normal stress exerted on the failure surface
τ^*	Dimensionless form of the tangential stress
σ_n^*	Dimensionless form of the normal stress
ψ	Dilatancy angle
χ and k	Parameters of a general equation of linear type of the flow rule
ζ	Coefficient of toughness of the original HB failure criterion
ζ_a	Coefficient of toughness of the generalized HB failure criterion
μ	Mean value of the FS

Introduction

The estimation of the factor of safety (FS) value in rock slope stability is one of the most important tasks for the design of different geotechnical works, i.e. infrastructures, mining, dams, etc.

The most widely used failure criterion in the study of the behaviour of rock masses is the generalized non-linear empirical Hoek–Brown (HB) criterion (Hoek et al. 2002; Hoek and Brown 2019). This failure criterion is widely accepted for the study of homogeneous and isotropic types of rock media as an equivalent continuum, which includes weak rock mass and heavily fractured rock mass where the governing failure pattern is along a rotational failure surface rather than through intact rock and joints.

In the state of the art of rock slope stability analysis, both by limit equilibrium method (LEM) and finite element method (FEM), the Mohr–Coulomb (MC) linear failure criterion is still the most widely used one considering that the material strength is expressed in terms of normal and shear stresses rather than in terms of principal stresses. In the past, most of the commercial numerical software did not use the HB failure criterion, and for this reason, the need arose to know the equivalent MC shear strength parameters (cohesion and friction angle) of the rock mass deduced from the HB criterion that should depend on the

range of confining stress ($\sigma\prime_{3max}$) governing the results of analysis. Nowadays, modern commercial software has introduced the HB criterion; therefore, it seems unnecessary to continue using the equivalent MC parameters, although the conversion of the parameters is still used for many geotechnical applications. For the equivalent parameters to be valid, it is important to choose the appropriate stress range for the failure mechanism depending on the geotechnical problem at hand. There are a lot of proposals for the estimation of equivalent MC parameters for tunnelling problems (Hoek et al. 2002; Sofianos 2003; Sofianos and Nomikos 2006; Jiménez et al. 2008), rock slope stability (Hoek et al. 2002; Yang and Yin 2010; Li et al. 2008; Wei et al. 2018, Rafiei Renani and Martin 2020), strip footing on rock mass (Yang and Yin 2010), etc. Anyway, the majority of the proposed solutions for determination of equivalent MC parameters provide great discrepancies due to different estimations of confining stress level ($\sigma\prime_{3max}$).

The plasticity flow rule describes the relation between the plastic strain increment and stress tensor following yielding. The associative flow rule is the condition for which the normality criterion is satisfied (e.g. for MC criterion dilatancy angle is equal to friction angle). In the slope stability analysis of homogeneous and isotropic rock mass obeying HB failure criterion, the flow rule is usually not well defined. In the study performed by Melentijevic (2005) and Melentijevic et al. (2017), the analysis of the influence of flow rule on rock slope stability is studied in detail. These results confirm the overestimation of FS by the application of the hypothesis of the associative flow rule in comparison to the non-associative flow rule with the corresponding dilatancy angle (ψ) depending on the rock mass quality.

Also, another problem arises in FEM considering that stability problems are based on the shear strength reduction technique (SSR method) where the values of cohesion and friction angle ($c\prime and \phi\prime$) are reduced by an iterative process until reaching the FS. Further on, as a consequence of strength envelope linearization over the stress range of interest, the same material can have different equivalent shear strength parameters ($c\prime and \phi\prime$). In this paper, the implication of stress-dependent linear parameters is analysed from the vertical cut slope perspective (upper and lower bound solution).

There are a lot of charts still being elaborated and used by many researchers for the preliminary quick assessment of the stability of rock slopes (Hoek and Bray 1981; Carranza-Torres 2004; Melentijevic 2005; Jiménez et al. 2008; Li et al. 2008; Li et al. 2009; Li et al. 2011; Shen et al. 2013; Melentijevic et al. 2017; Zuo and Shen 2020; etc.). In this study, the stability of the rock slope presented is evaluated by taking into account different flow rules introduced in the generalized HB criterion.

Nowadays, probabilistic slope stability assessment is often used to address uncertainties originating from input parameters. In recent years, many researchers have studied different probabilistic aspects applied to rock slope stability (e.g. Serrano and Castillo 1973; Griffiths and Fenton 2004; Zhang et al. 2010; Javankhoshdel and Bathurst 2016; Javankhoshdel et al. 2017; Zhou et al. 2017; Rafiei Renani et al. 2019; Wang et al. 2020; Guo et al. 2020; Johari et al. 2020). Probabilistic and statistical concepts are implemented in Eurocodes (in particular Eurocode 7—European standard for geotechnical design), where, for example, characteristic values of geotechnical parameters could be determined by statistical procedures (Tietje et al. 2014). The analysis considered in this study is extended to account for the probability of failure for associative and non-associative flow rules. For the considered case study, when the slope stability analysis is performed under the assumption of the associative flow rule, the probability of failure is within acceptable limits, while under the non-associative flow rule, the probability of failure is rather high, whereas the deterministic factor of safety is close to unity.

For the application of the HB criterion, it is important to take into account the uncertainty in the estimation of basic input parameters σ_{ci}, GSI and m_i and its effect on the study of a particular geotechnical problem. For that purpose, sensitivity analysis is performed to produce charts for the analysed case study showing the range of input parameters within the realistic values of parameters for rock material considered (σ_{ci}, GSI and m_i) for associative and non-associative flow rule that would lead to failure of rock slope.

Failure criterion

Hoek and Brown failure criterion

The HB failure criterion (2002, 2019) is the empirical criterion most widely used in rock mechanics, based on the GSI classification system. Its applicability to the rock mass considers intact rock, blocky, and heavily jointed rock mass (Fig. 1). These groups can be considered homogeneous and isotropic, i.e. mainly applicable to soft and highly fractured rocks.

The formulation of the latest version of the HB criterion, which has undergone different modifications throughout its development, is the following:
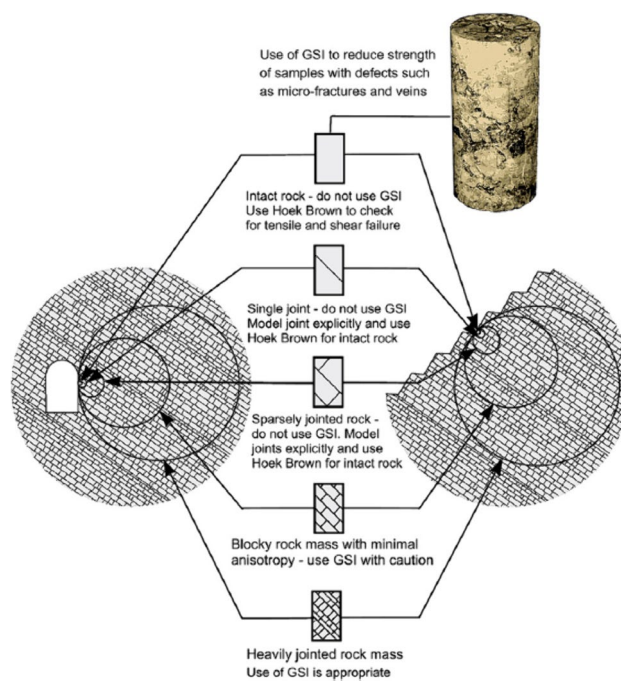

Fig. 1 Scale effect and applicability of the HB failure criterion (modified after Hoek and Brown 2019)

$$\sigma'_1 = \sigma'_3 + \sigma_{ci}\left(m_b \frac{\sigma'_3}{\sigma_{ci}} + s\right)^a \tag{1}$$

where σ'_1 and σ'_3 are the major and minor principal stresses at failure; σ_{ci} is the uniaxial compressive strength of the intact rock; m_b is the reduced value of the intact rock mass constant m_i; and s and a are the rock mass material constants. Where:

$$m_b = m_i \exp\left(\frac{GSI - 100}{28 - 14D}\right) \tag{2}$$

$$s = \exp\left(\frac{GSI - 100}{9 - 3D}\right) \tag{3}$$

$$a = \frac{1}{2} + \frac{1}{6}\left(e^{-GSI/15} - e^{-20/3}\right) \tag{4}$$

Deformation modulus of the rock mass is defined based on the availability of data on the elastic modulus of intact rock (E_i):

$$E_{rm}(MPa) = 100000\left(\frac{1 - D/2}{1 + \exp((75 + 25D - GSI)/11)}\right) \text{ or } E_{rm} = E_i\left(0.02 + \frac{1 - D/2}{1 + \exp((60 + 15D - GSI)/11)}\right) \tag{5}$$

where *GSI* is the geological strength index, and *D* is the disturbance factor taking into account the effect of blasting and stress relaxation (varying from 0 for undisturbed rock mass to 1 for completely disturbed rock mass) (Hoek and Brown 2019).

Rafiei Renani and Cai (2022) comprehensively reviewed the evolution of the HB criterion and emphasized its advantages and disadvantages and the effect of parameter uncertainty on the reliability of estimated rock mass properties.

Shear/normal function of HB failure criterion

The HB criterion can be presented alternatively as a shear/normal function as given in Serrano and Olalla (1994) for the original HB (Hoek and Brown 1980) and by Serrano et al. (2000) for the generalized HB (Hoek et al. 1992).

The stresses exerted on the failure surface (Coulomb type failure criterion) can be parametrically obtained from the Mohr failure criterion type (envelope of stress circles), setting the value of the instantaneous friction angle (ϕ) as a parameter, defined as the slope of Mohr's envelope. These stresses (τ and σ), referred to the point R representing the state of stress exerted on the failure plane (Fig. 2), in the dimensionless form (τ^* and σ_n^*), are given according to:

$$\tau^* \equiv \tau/\beta_a = q^*(\phi)\cos\psi \tag{6}$$

$$\sigma_n^* \equiv \sigma_n/\beta_a = p^*(\phi) - q^*(\phi)\sin\psi \tag{7}$$

A general flow rule for rock masses, which is necessary to define a Coulomb type failure criterion can be of linear type, establishing the relation between the instantaneous friction angle (ϕ) with the dilatancy angle (ψ):

$$\sin\psi = \chi \cdot \sin\varphi + k \tag{8}$$

where χ and k are the parameters of a general equation of linear type.

Specific cases of this general flow rule given in Eq. (8) are: (a) the associative rule with $\chi = 1$ and $k = 0$ that gives a dilatancy angle equal to instantaneous friction angle ($\psi \equiv \phi$) and (b) the non-associative rule with a constant value of dilatancy angle ($\psi \equiv \psi_0$) for $\chi = 0$ and $k = \sin\psi_0$.

When analysing rock slope stability in two-dimensional form, the case is of the plane strain. The HB failure criterion can be simplified using Lambe's variables ($p = (\sigma_1 + \sigma_3)/2$,$q = (\sigma_1 - \sigma_3)/2$), which is given in the dimensionless form ($p_0^* = p/\beta_a + \zeta_a$ and $q^* = q/\beta_a$) in Serrano et al. (2000):

$$\frac{p}{\beta_a} + \zeta_a = \left[1 + (1-a)\left(\frac{q}{\beta_a}\right)^k\right]\frac{q}{\beta_a} \tag{9}$$

which becomes:

$$p_0^* \equiv p^* + \zeta_a = \left[1 + (1-a)q^{*k}\right]q^* \tag{10}$$

Parameters β_a and ζ_a are two basic material constants that establish the rock strength, based on the HB parameters a, m_i, and s as well as on the uniaxial compressive strength of the intact rock (σ_{ci}) as follows:

$$\beta_a = A_a\sigma_{ci} \tag{11}$$

$$\zeta_a = s/(m_b A_a) \tag{12}$$

where

$$k = (1-a)/a \text{ and } A_a^k = m_b(1-a)/2^{1/a} \tag{13}$$

The strength modulus β_a is used to scale the failure criterion, while the coefficient of toughness ζ_a represents the relative quality and strength of the rock mass; i.e., it inherits the type of rock mass and extent to which it is fractured and disturbed representing the "dimensionless isotropic tensile strength" of the rock mass and can be regarded as the "tensile strength coefficient of the rock mass".
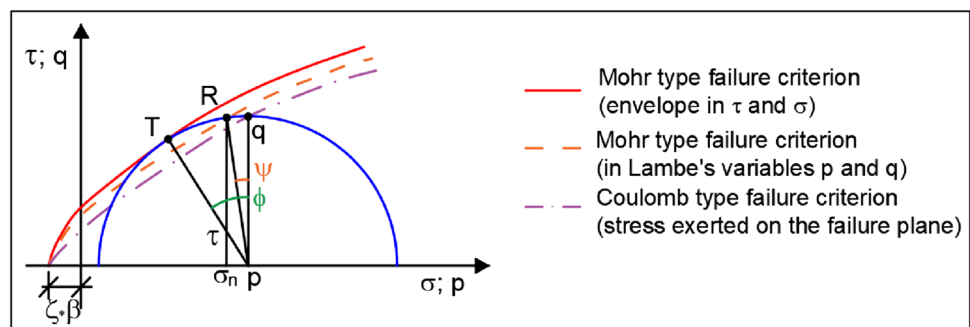
The instantaneous friction angle (ϕ) is defined as the tangent line of the Mohr's envelope expressed as:

$$\sin\rho = dq^*/dp_0^* = 1/\left(1 + kq^{*k}\right) \tag{14}$$

Depending on the instantaneous friction angle (ϕ), Lambe's dimensionless variables that follow the HB criterion are as follows:

$$q^* \equiv q/\beta_a = \left[\frac{1 - \sin\phi}{k\sin\phi}\right]^{1/k} \tag{15}$$

Fig. 2 Types of failure criteria (modified from Serrano et al. 2005)

- Mohr type failure criterion (envelope in τ and σ)
- Mohr type failure criterion (in Lambe's variables p and q)
- Coulomb type failure criterion (stress exerted on the failure plane)

$$p_0^* \equiv p/\beta_a + \zeta_a = a \left[\frac{1 + k\sin\phi}{\sin\phi}\right] \left[\frac{1 - \sin\phi}{k\sin\phi}\right]^{1/k} \qquad (16)$$

The advantage of representing the shear/normal stress function in this form is that it does not require the range of principal stresses to be determined for its application in the analysis of slope stability.

Associative and non-associative flow rule

In the slope stability analysis of rock masses obeying the HB failure criterion for homogeneous and isotropic rock mass, the application of the associative flow rule results in an overestimation of the FS in comparison to the analysis with the application of the non-associative flow rule (Melentijevic 2005; Melentijevic et al. 2005, 2017). The usually proposed and applied values of dilatancy angle (ψ) in the non-associative flow rule for different geotechnical problems are conditioned by the rock mass quality defined by GSI and the friction angle (ϕ'), being defined: for poor-quality rock mass (GSI = 25) $\psi = 0°$, for average-quality rock mass (GSI = 50) $\psi = 4°$ ($\phi'/8$), and for good-quality rock mass (GSI = 75) $\psi = 11.5°$ ($\phi'/4$), as proposed by Hoek and Brown (1997), although other types of the general flow rule can be proposed.

Other studies included the analysis of the flow rule by the introduction of the dilatancy angle such as those given for infinite rock slopes (Manzanas 2002; Serrano et al. 2005) and planar failure (Serrano et al. 2002; Serrano and Olalla 2004; Melentijevic 2005; Melentijevic et al. 2006).

The influence of the flow rule on other geotechnical problems in rock mechanics is given for tunnelling (Reig 2004; Alejano and Alonso 2005; Serrano et al. 2011), anchors (García Wolfrum, 2005), footings on rock mass (Alencar et al. 2019, 2021), etc., confirming the importance for incorporation of non-associative flow rule into the analysis.

Equivalent Mohr–Coulomb failure parameters

Different commercial geotechnical software still widely uses the linear MC criterion for the analysis of different geotechnical problems making this methodology a general engineering approach. For that purpose, it is necessary to obtain values of equivalent MC parameters, i.e. c' and ϕ', by the linearization of Eq. (1) in the range of minor principal failure stress $\sigma_1' < \sigma_3' < \sigma_{3max}'$ (Fig. 3) (Hoek et al. 2002):

$$\varphi' = \sin^{-1}\left[\frac{6am_b(s + m_b\sigma_{3n}')^{a-1}}{2(1+a)(2+a) + 6am_b(s + m_b\sigma_{3n}')^{a-1}}\right] \qquad (17)$$
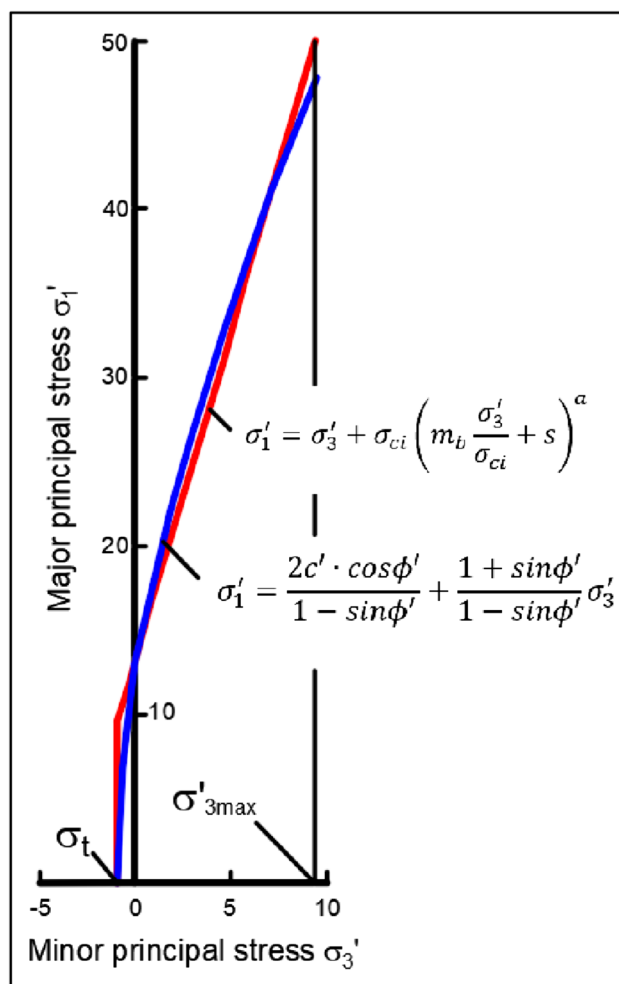

Fig. 3 Relation between major and minor principal stress at failure of the HB criterion and equivalent MC parameters (Hoek et al. 2002)

$$c' = \frac{\sigma_{ci}\left[(1 + 2a)s + (1 - a)m_b\sigma_{3n}'\right] \cdot \left(s + m_b\sigma_{3n}'\right)^{a-1}}{(1+a)(2+a)\sqrt{1 + \left(6am_b(s + m_b\sigma_{3n}')^{a-1}\right)/((1+a)\cdot(2+a))}} \qquad (18)$$

where $\sigma_{3n}' = \sigma_{3max}'/\sigma_{ci}$, and σ_t tensile strength.

The value of σ_{3max}' is the upper limit of the confining stress for which the relationship between the MC and the HB failure criteria is considered, and it should be defined for various geotechnical applications (tunnels, slopes, foundations, etc.). The determination of the value of σ_{3max}' in the case of slopes must correspond to the adjustment of the value of the FS against slope failure, including the shape and location of the failure line. Hoek et al. (2002) proposed the following relationship determined for different ranges of slope geometries and rock mass properties based on Bishop's method:

$$\frac{\sigma_{3\max}\prime}{\sigma_{cm}\prime} = 0.72 \left(\frac{\sigma_{cm}\prime}{\gamma H} \right)^{-0.91} \tag{19}$$

where γ and H are the unit weight and the slope height, respectively; $\sigma_{cm}\prime$ is the rock mass compressive (or "global") strength, defined by the following Eq. (20), for the stress range $\sigma_t < \sigma_3\prime < \sigma_{ci}/4$ (Hoek et al. 2002):

$$\sigma_{cm}\prime = \sigma_{ci} \frac{\left(m_b + 4s - a(m_b - 8s) \right) \cdot \left(m_b/4 + s \right)^{a-1}}{2 \cdot (1 + a) \cdot (2 + a)} \tag{20}$$

Li et al. (2008) have defined three zones as can be seen in Fig. 4. If the stress conditions of the rock material fall within zones 1 and 3, overestimation of the ultimate shear strength can be considered using the equivalent MC parameters instead of the HB curve.

According to Li et al. (2008), for very steep slopes, the stresses along the failure surface fall within the zone 1 (Fig. 4), producing the maximum difference between the HB and MC failure criterion. Therefore, the shear stress obtained using the HB criterion is less than that obtained using the MC criterion by applying Eq. (19).

A better adjustment of the equivalent parameters is required in order not to overestimate the FS, especially on slopes with an angle of inclination (δ) greater than 45° (Li et al. 2008). The following modified formulations are proposed based on the slope inclination angle (δ), to try to provide a better fit of the linearization of the HB curve in zone 1 (Fig. 4):

$$\frac{\sigma_{3\max}\prime}{\sigma_{cm}\prime} = 0.2 \left(\frac{\sigma_{cm}\prime}{\gamma H} \right)^{-1.07} \delta (\geq 45°) \tag{21}$$

$$\frac{\sigma_{3\max}\prime}{\sigma_{cm}\prime} = 0.41 \left(\frac{\sigma_{cm}\prime}{\gamma H} \right)^{-1.23} (\delta < 45°) \tag{22}$$

Rafiei Renani and Martin (2020) performed numerical analysis for over 100 slopes to investigate the influence of $\sigma_{3\max}\prime$ on FS and failed material area by applying the proposed original HB Eq. (19) and modified Eqs. (21) and (22). Based on numerical analysis, they obtained the following relation between $\sigma_{3\max}\prime$ and slope angle (δ):

$$\frac{\sigma_{3\max}\prime}{\gamma H} = \frac{0.175}{\tan(\delta)} \tag{23}$$

Anyway, the best adjustment of the value of the minor principal stress $\sigma_{3\max}\prime$ considering the analysis of the non-linear correlation of the HB failure criterion and the derived equivalent MC parameters should correspond to the maximum thickness of the failed material area.

Applied methodology

Charts

Chart-based slope stability analysis is still widely used in everyday practice for the quick estimation of the geometry of the slope based on geotechnical parameters. The most used stability chart for slope stability is presented by Taylor (1937) which requires the MC shear resistance parameters. There are different stability charts presented for rock slope design, such as Hoek and Bray (1981) that uses equivalent MC parameters, as well as others that use generalized HB failure criterion (Carranza-Torres 2004, Jiménez et al. 2008, Li et al. 2008, Li et al. 2009, Li et al. 2011, Zuo and Shen 2020; Kumar et al. 2021). The charts presented by Melentijevic (2005) and Melentijevic et al. (2017) incorporate different assumptions of flow rules in the HB failure criterion. These charts were developed for the original HB criterion (1980) applying the parametric form of shear/normal stress given by Serrano and Olalla (1994), taking into account different flow rules. If the associative flow rule is applied by these charts, the slope stability (i.e. the general slope angle) is overestimated in comparison to the application of the non-associative flow rule. An example of the application of these charts is presented in Fig. 5 confirming the influence of different flow rules on results by the estimation of the necessary slope angle for FS = 1.0.
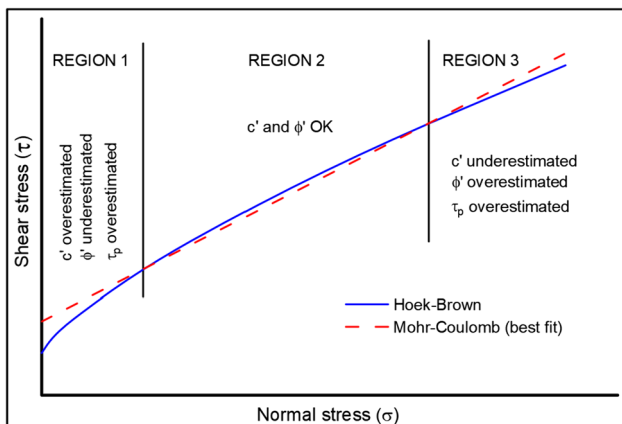

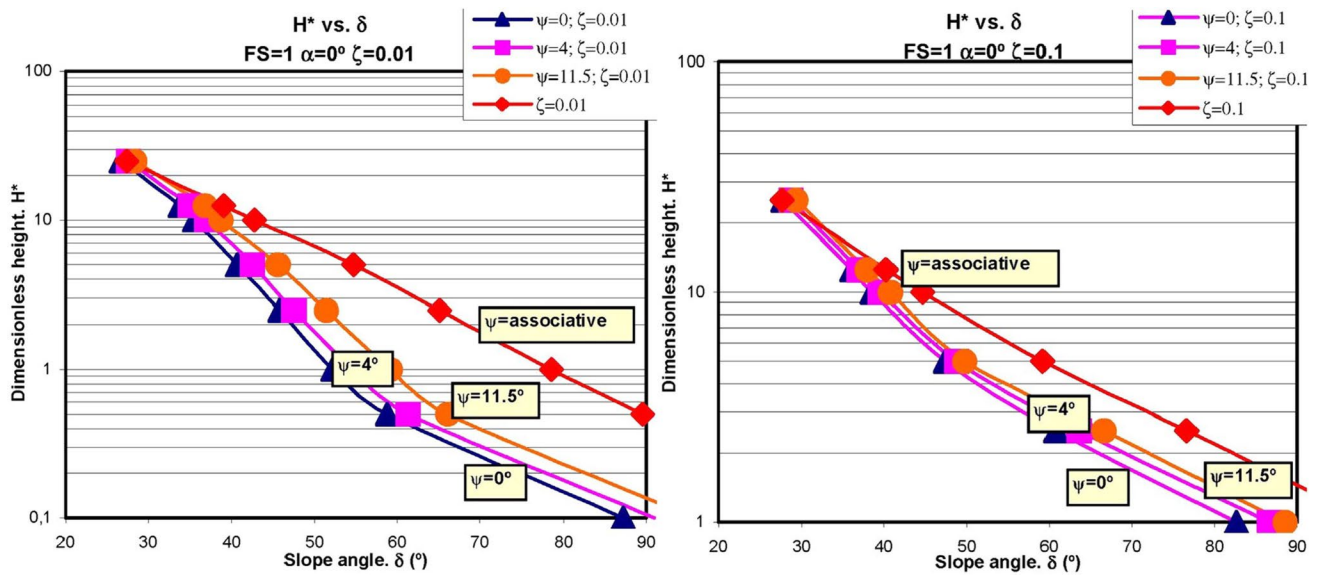**Fig. 4** Linearization of the HB failure criterion (Li et al. 2008)

Fig. 5 Relationship between dimensionless height (H*) and slope angle (δ) for FS = 1.0 and different flow rules with constant values of ψ for **a** ξ =0.01 and **b** ξ=0.1 (Melentijevic et al. 2017)

Limit equilibrium method

The LEM is the most widely used and preferred method for slope stability, due to its simplicity (compared to the more rigorous approaches such as FEM) and good understanding of its outcomes. The commercial code Slide2 v9.020 (RocScience 2022a) is used for the analysis in this study. The location of the critical failure surface with the lowest FS value is determined by the automated grid search for the general circular failure surface. The Morgenstern-Price method is used which satisfies both the equilibrium of forces and moments (Morgenstern and Price 1965).

Critical slope height

The vertical cut problem is well known within the framework of the theory of plasticity, namely the collapse load theorem. This theorem can produce upper and lower bound solutions to the problem at hand and is usually termed limit analysis. The well-known equation to determine a lower bound solution for critical height H_L of vertical cut (Davis and Selvadurai 2002) is the following:

$$H_L = \frac{2c}{\gamma} \sqrt{N} \tag{24}$$

where N is defined as: $N = \frac{1+\sin\phi\prime}{1-\sin\phi\prime}$

Upper bound solution for critical height H_U of vertical cut (Davis and Selvadurai 2002) is:

$$H_U = \frac{4c}{\gamma} \sqrt{N} \tag{25}$$

Finite element method

The commercial code RS2 v11.013 (Rocscience Inc. 2022) is used for FEM analysis. The location of the failure surface is automatically determined by the analysis of deformations, i.e. the maximum shear strains, without a requirement to make any hypothesis on the shape and position of the failure surface.

The initial stress field is considered by the gravity loading option. The adopted initial value of lateral earth pressure coefficient (K_0) is 1.0, considering the findings from the study done by Rafiei Renani and Martin (2020). The deformation modulus is introduced according to Eq. (5). It should be noted that it has no influence on the value of FS, as previously discussed by different authors (Cheng et al. 2007; Griffiths and Lane 1999; Hammah et al. 2005).

The lateral boundaries of the model are sufficiently large in order not to influence the results of analysis. Left- and right-side model boundaries are restrained only in the y-direction, while the bottom boundary is completely restrained (x- and y-direction). The uniform mesh with 6-noded triangular elements (total no 2767 elements) is used.

When the generalized HB criterion is applied, the associative and non-associative flow rule is introduced by the value of the dilation parameter (m_{dil}), ranging from 0 for

the non-associative flow rule with $\psi = 0°$ ($m_{dil} = 0$) to m_b for the associative flow rule ($m_{dil} = m_b$) (Rocscience Inc. 2022, Naznin 2007).

When an equivalent linear MC criterion is used, the associative flow rule is introduced by the equivalence of the dilation to the friction angle ($\psi = \phi$) and the non-associative flow rule by ψ=variable.

The FS is determined by the SSR method which reduces the shear strength until instability occurs. The application of the SSR method for the MC criterion (by the introduction of equivalent parameters) includes the iterative application of FS on shear strength parameters (c and ϕ). It is supposed that in both cases of associative ($\psi = \phi$) and non-associative flow (ψ=variable) rule the same FS is applied during the iterative process on the dilatancy angle (ψ).

In the case of the HB failure criterion, the SSR method is introduced based on the formulation presented by Benz et al. (2008), in which an intrinsic shear strength factor is included in the shear strength criterion.

When the shear/normal function is introduced to define the failure criterion, it permits the introduction of arbitrary function and the construction of a non-linear MC strength envelope. In this case, shear/normal function is introduced by Eqs. (6) and (7) that already involve the flow rule, thus being unnecessary to introduce the dilation parameter (m_{dil}). The SSR method is applied directly to the value of shear strength (Rocscience Inc. 2022b).

Probabilistic analysis

In the next step, a reliability analysis was performed to investigate the influence of applied flow rule on the probability of failure (P_f). In terms of universal definition, the P_f is the likelihood that the structure will fail during operational life and is an important part of risk analysis. The P_f, calculated together with the consequence of failure (CoF), helps in establishing the risk level for a particular problem at hand.

In slope stability analysis, P_f is defined as (Rocscience Inc. 2022a):

$$P_f = (total\,no.\,of\,analyses)/(no.\,of\,analyses\,with\,FS < 1.0) \tag{26}$$

Another commonly used measure of safety in probabilistic analysis is the reliability index (*RI*) which is defined, for an assumption of normal distribution of FS after probabilistic analysis, as follows:

$$RI = \frac{\mu - 1}{SD} \tag{27}$$

where μ is mean value of the FS and *SD* is standard deviation of FS.

As can be seen from Eq. (27), the RI represents the number of standard deviations that separate the mean FS from the critical FS.

For an assumption of lognormal distribution of FS, the RI can also be determined.

Before analysis, one has to assign a statistical distribution to random variables (input parameters). In the case of MC failure criterion, random variables usually represent shear strength parameters (c′ and ϕ′).

However, in the case of nonlinear criterion, namely shear/normal function, statistical distribution has to be assigned directly to the shear strength of the material. In this way, the variation of shear strength in the analysis is defined by the coefficient of variation (CoV). The CoV is the ratio of the SD to the mean value and shows the extent of variability to the mean of the population. The higher CoV implies greater dispersion, and vice versa. According to Eurocode 7 (EN 2004), CoV for shear strength of material varies in the range of 15 to 25%, being in this study the value of CoV = 20% assumed.

Regarding the number of analysed failure surfaces, two different probability analyses could be performed, namely the *Overall slope* and *Global minimum*. In the case of global minimum analysis, probability of failure is determined only for critical deterministic failure surface. Therefore, the P_f and the RI are only based on the analysis of one slip surface. For the Overall slope method, the entire slip surface search is repeated within a prescribed number of samples. In this case, each iteration of the probabilistic analysis can locate a different global minimum slip surface.

After defining random variables, and their distributions, the sampling method has to be determined. The sampling method determines how the statistical input distributions for the random variables will be sampled. The theoretical background of these methods can be found in Robert and Casella 2004; El-Ramly et al. 2002; McKay et al. 1979; and Iman et al. 1980. Three sampling techniques are available in software, namely *Monte Carlo simulation*, *Latin Hypercube technique*, and *Response surface*. It is important to mention that the Latin Hypercube sampling technique gives comparable results to the Monte Carlo technique but with fewer samples. This is why the Latin Hypercube sampling technique is chosen in this study.

Case study of failed slope

The case study analysed is presented by Berisavljevic et al. (2018). The slope is 12 m high with a uniform inclination of 45°. During highway construction, the failure occurred. The rock mass is classified as poor-quality mudshale. Groundwater was not detected during and after geotechnical investigations, so the analysis is performed without consideration of

Fig. 6 Uniform homogeneous slope in mudstone rock mass (Berisavljević et al., 2018)
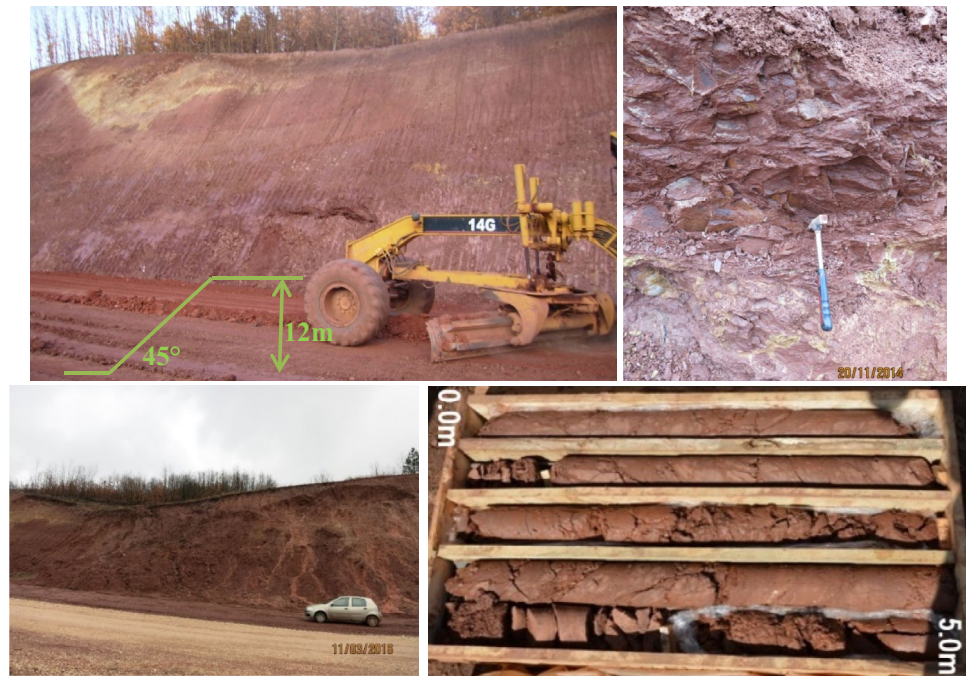
pore-water pressures. The geometry of the slope and view of the mudstone material is shown in Fig. 6.

Table 1 summarizes geotechnical parameters of the material defined in situ and derived by formulations presented in Serrano et al. (2000) and Melentijevic (2005) (see the "Failure criterion" section), which are further necessary for the analysis performed by charts, LEM, FEM, and probabilistic and sensitivity analyses.

The constant value of disturbance factor of $D = 0.7$ is assumed (mechanical excavation due to stress relaxation according to Hoek and Brown 2019) in the whole model. Other assumptions on the distribution of disturbance factor D are possible, i.e. different linearly varying distribution, according to Silva-Guzmán and Gómez (2015), Rose et al. (2018), and Ma et al. (2022), but this assumption of constant value of D is considered to be on the safe side from the practical point of view.

In the following section, results of analyses, considering the influence of flow rules, are shown.

At first, the preliminary estimation of slope stability by application of charts given in Melentijevic (2005) and Melentijevic et al. (2017) is performed. Nevertheless, as expected, the original HB overestimates the rock mass strength, so the evaluation of the stability of the rock slope is performed additionally to take into account the generalized HB criterion. Then, the FEM and LEM analyses with generalized HB criterion in its parametric form (Serrano et al. 2000; Melentijevic 2005) are discussed. The comparison is made between the results obtained with generalized HB and equivalent MC criteria both in LEM and FEM. The dependence of the MC parameters on the $\sigma_{3max}\prime$ level (refer to the "Application of equivalent MC

parameters" section) is used to analyse the vertical cut problem, common for limit analysis. The probabilistic analysis is performed to investigate the influence of different flow rules on the probability of failure. Finally, the sensitivity analysis is done to obtain the failure charts applicable to this case study. These failure charts reproduce a combination of HB parameters (namely m_i, σ_{ci}, and GSI), derived from a shear/normal function, that would lead to the failure of analysed slope, both for associative and non-associative flow rule.

Results and discussion

Application of charts

For preliminary analysis of slope stability, the dimensionless charts presented in Fig. 5 are used. These charts are also used to evaluate the influence of the flow rule on results by the estimation of the necessary slope angle for FS = 1.0. Considering that graphs are developed for particular values of ζ(0.01 and 0.1), the interpolation is done to match the value given in Table 1 for the analysed case study. The overestimation of the slope angle can be observed if the associative flow rule is adopted, while the non-associative flow rule with $\psi = 0°$ (corresponding to poor quality of the rock mass) matches approximately limit equilibrium for the existing adopted geometry of the case study, as summarized in Table 2. It can be observed from Fig. 5 that in general, the application of the associative flow rule represents the unconservative approach in the rock slope stability analysis.

Application of equivalent MC parameters

Table 3 summarizes the results of LEM and FEM by employing equivalent MC parameters (c′ and ϕ′) determined by different authors (chapter "Equivalent Mohr–Coulomb failure parameters"). To simulate the associative and non-associative flow rule in FEM, the value of the dilation angle (ψ) is introduced either by ψ=ρ (associative) or ψ = 0° (non-associative).

From Table 3, it can be observed that the shear strength parameters (c′ and ϕ′), obtained for different $\sigma_{3max}\prime$ values, have significant influence on the factor of safety. The greater the $\sigma_{3max}\prime$, the greater the FS. If the result calculated for the non-associative flow rule by FEM (Eq. 21) is considered as reference (FS = 1.58), all other assumptions provide errors in the estimation of FS. The maximum difference is up to 12.72%.

Additional analyses are performed to investigate the influence of the K_0 value on $\sigma_{3max}\prime$. The K_0 is varied from 0.5 to 3.0, which is considered the common range for rock slope engineering problems. Depending on the position of the critical sliding surface from LEM (obtained for shear/normal function of the HB criterion under associative flow rule assumption), $\sigma_{3max}\prime$ varied from 41 and 70 kPa for $K_0 = 0.5$ and 3.0, respectively. The critical sliding surface obtained in LEM by the application of shear/normal function with non-associative flow rule is much shallower (refer to section "Application of HB criterion") producing $\sigma_{3max}\prime$ values between 26 and 35 kPa, for $K_0 = 0.5$ and 3.0, respectively. Even though the selection of K_0 produces differences, they are not considered significant from the practical point of view. These findings are in agreement with the conclusions of Rafiei Renani and Martin (2020).

Analysis of critical slope height

As shown in Table 3, the same material can have different shear strength parameters (c′ and ϕ′) based on proposed formulations by different authors. Shear strength parameters are also dependent on strength envelope linearization over the stress range of interest.

In the following, the dependence of shear strength on the stress level will be used to investigate its influence on the critical height of vertical cut.

For different sets of c′ and ϕ′ parameters from Table 3, critical cut heights H_L and H_U are calculated and presented in Table 4 and Fig. 7.

The exact collapse height for this problem, if we assume that the material cannot support tension, is precisely equal to H_L. If we assume that the material cannot support tensile stress, then a vertical tension crack can develop behind the cut's face and, rather than the failure wedge, a thin slab of soil can collapse leaving a new, near vertical face. If the material supports tension, then H_U will be closer to the true collapse load. The reason H_U is twice the exact value of H_L is due to the choice of collapse mechanism (planar failure surface) (Davis and Selvadurai 2002).

Collapse load theorems were originally developed for elastic-perfectly plastic materials that obey the associative flow rule. Regardless of this, one can try to determine the vertical cut height (FS = 1.0) within the LEM framework.

It is well known that for the planar (wedge) failure surface LEM calculation will produce the vertical cut height identical to H_U (with the same c′/ϕ′ material considered). In the case of a lower bound solution, the H_L value should be matched to the LEM analysis by introducing a tension crack of a certain depth.

Fig. 7 Critical height of the vertical cut for different σ′$_{3max}$ levels
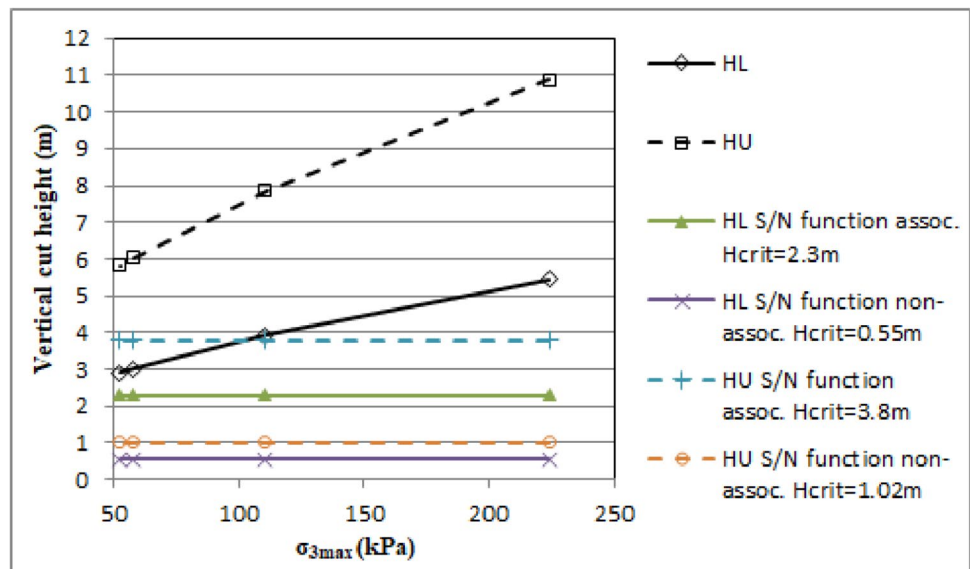
Next, one could try to determine the vertical cut height by introducing a nonlinear shear/normal function in LEM for the set of parameters summarized in Table 1. If a nonlinear strength envelope is applied, the critical height of the vertical cut is stress independent and should have constant value over the entire stress level.

Results of limit analyses (Eqs. (24) and (25)) and LEM analyses with nonlinear shear/normal function (for associative and non-associative flow rule with $\psi = 0°$) are reproduced in the form of a graph in Fig. 7.

As expected, the critical cut height for the nonlinear strength envelope has a constant value over the stress range of interest and is lower than the corresponding results of limit analysis.

Although this analysis seems rather simple, it leads to one very important conclusion. For realistic materials (for which shear strength parameters are stress dependent), critical cut height is variable and depends on the choice of strength parameters for a particular stress range. If the nonlinear nature of the strength envelope is employed in the analysis by LEM, constant critical cut height is obtained.

Application of HB criterion

Table 5 summarizes results obtained by the application of LEM and FEM under different hypotheses for the failure criterion and flow rule. If LEM and FEM calculations are performed by the application of shear/normal function under the hypothesis of associative and non-associative flow rule (Eqs. (6) and (7)), the higher values of FS are observed for the case of associative flow rule compared to the non-associative (with $\psi = 0°$). If the generalized HB criterion is applied considering the dilation parameter (m_{dil}), a small difference is observed in FS under the assumption of associative and non-associative flow rule. In general, the approximate error between FS values obtained under the hypothesis of associative and non-associative flow rule is in the order of 45%, considering that the reference value is the one with the minimum FS (the shear/normal function with non-associative flow in FEM).

The failure surfaces obtained by LEM and FEM are compared in Fig. 8. The FEM failure surfaces are represented by the maximum shear strain band, while the failure surfaces obtained by LEM are introduced as red lines in Fig. 8. In general, failure surfaces obtained by LEM for associative and non-associative flow rule cover less failure area than the ones obtained by FEM. It can also be observed that the position of failure surfaces (for the generalized HB criterion) obtained by LEM for associative flow rule matches quite well with the ones obtained by FEM. The failure surfaces for the non-associative flow rule in LEM are shallower than those of the associative flow rule.
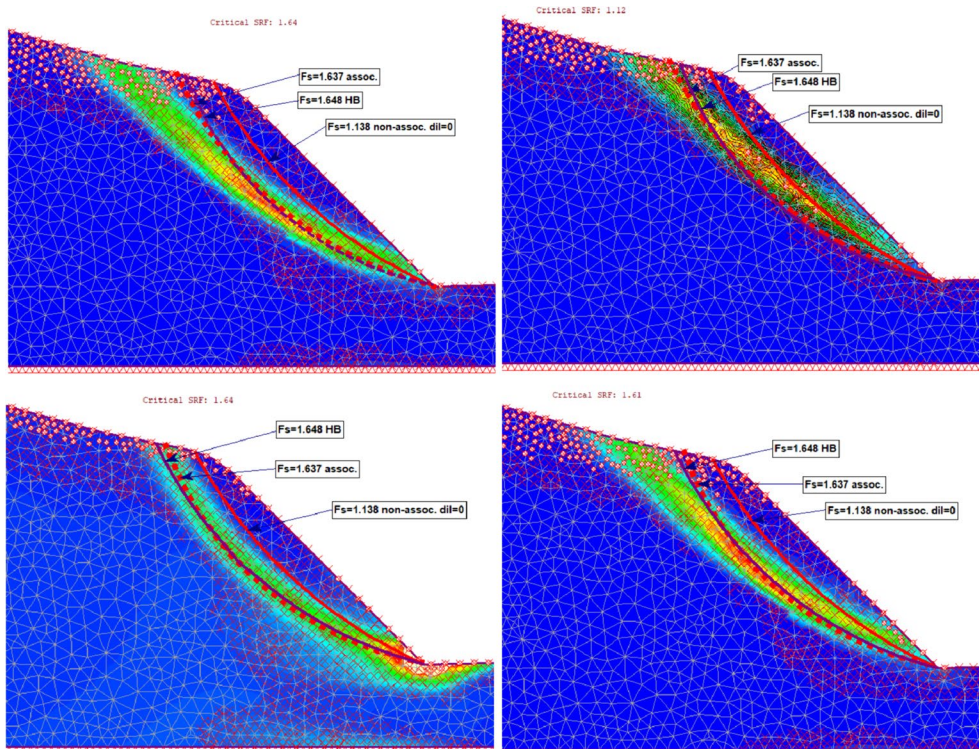

Fig. 8 Overlapped FEM vs LEM failure surfaces for **a** shear/normal function for associative flow rule, **b** shear/normal function for non-associative flow rule with $\psi = 0°$, **c** generalized HB with associative flow rule, and **d** generalized HB with non-associative flow rule with $m_{dil} = 0$
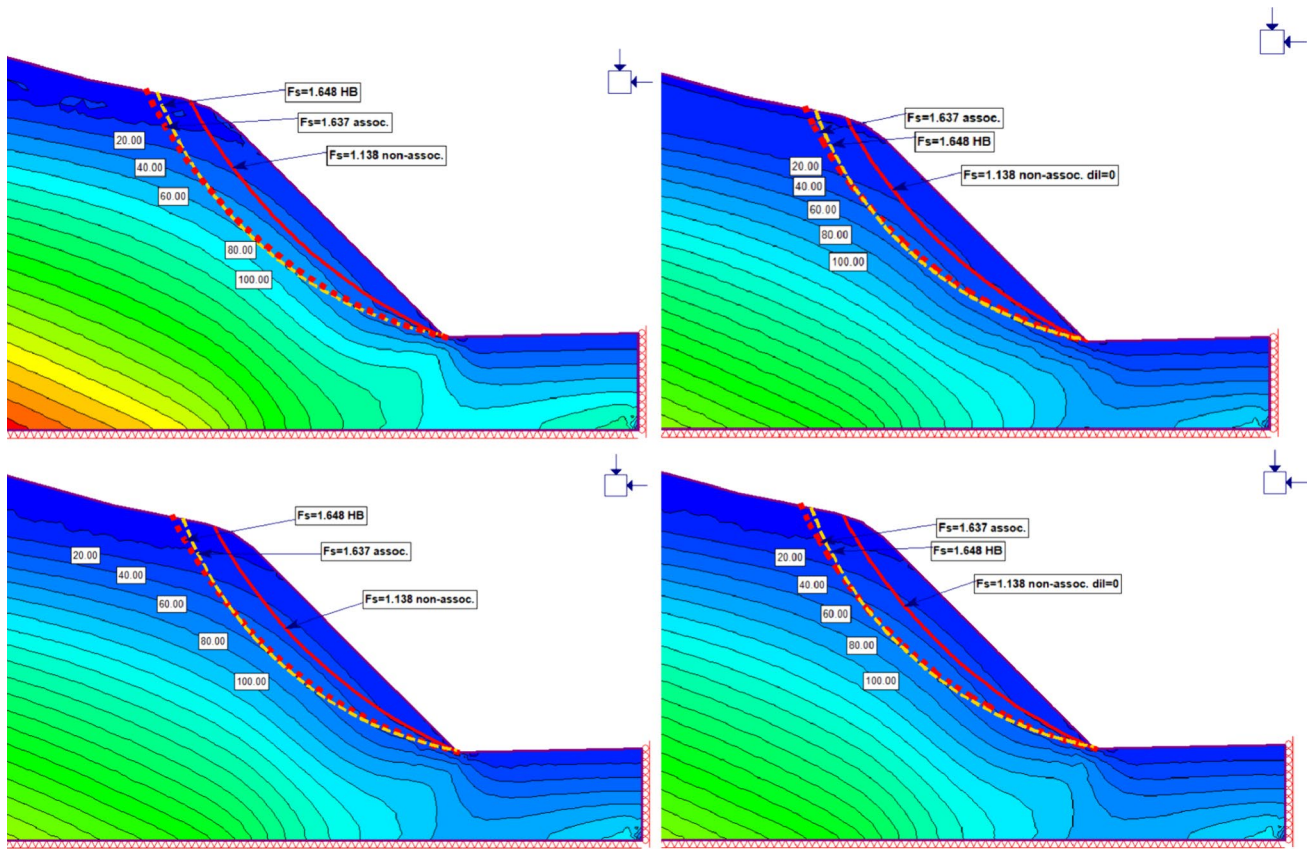
Fig. 9 FEM contours of minor principal stress (σ'_3) with the position of failure surfaces for **a** shear/normal function for associative flow rule, **b** shear/normal function for non-associative flow rule with $\psi = 0°$, **c** generalized HB with associative flow rule, and **d** generalized HB with non-associative flow rule with $m_{dil} = 0$

Figure 9 shows the contours of minor principal stress (σ'_3), obtained from FEM analysis, along with superimposed LEM failure surfaces for associative and non-associative flow rules. The σ_{3max}' value obtained by FEM is compared to the values obtained by different authors listed in Table 3. It can be observed that the value of σ_{3max}' (for $K_0 = 1.0$) ranges from 30 to 60 kPa under different assumptions of the non-associative and the associative flow rule, respectively. This is in accordance with the values provided by Rafiei Renani and Martin (2020) and Li et al. (2008) for $\delta \geq 45°$ (Table 3).
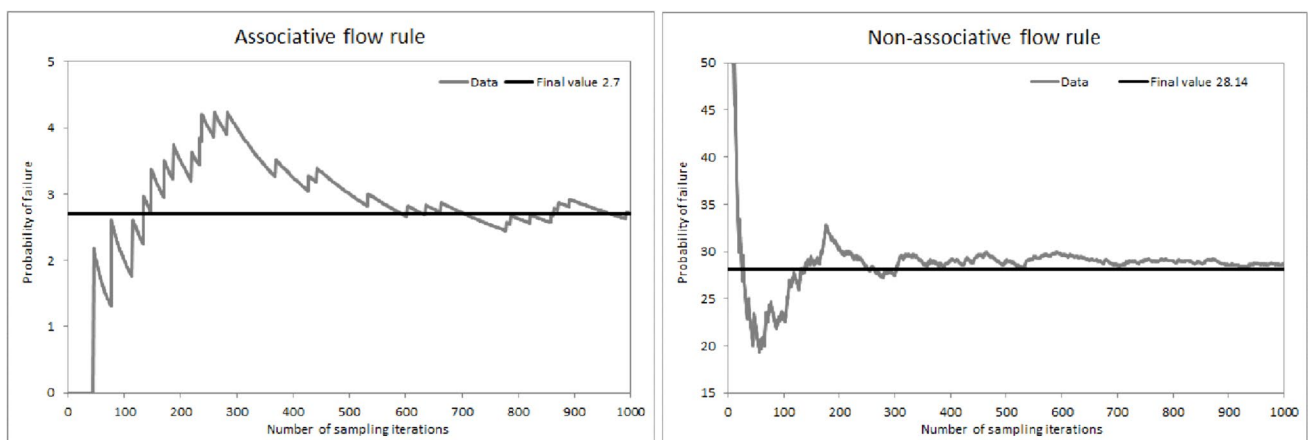
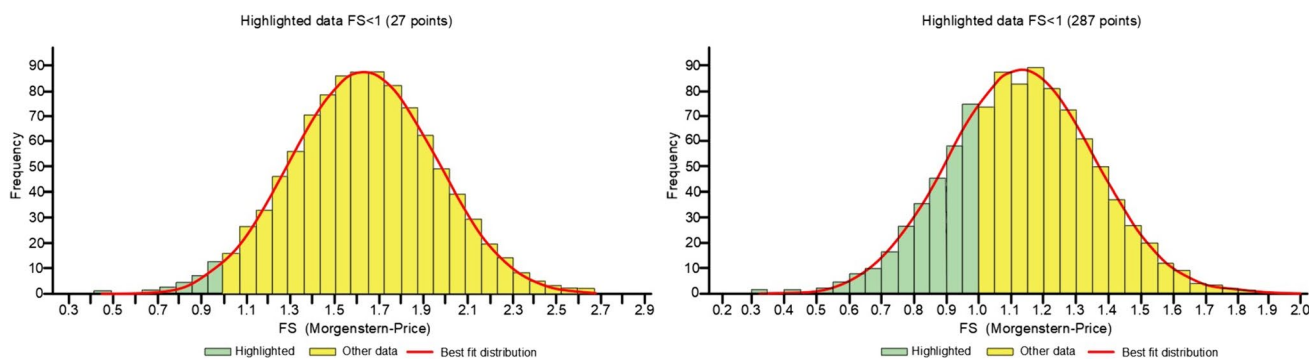**Fig. 10** P_f convergence plot for **a** associative and **b** non-associative flow rule with $\psi = 0°$

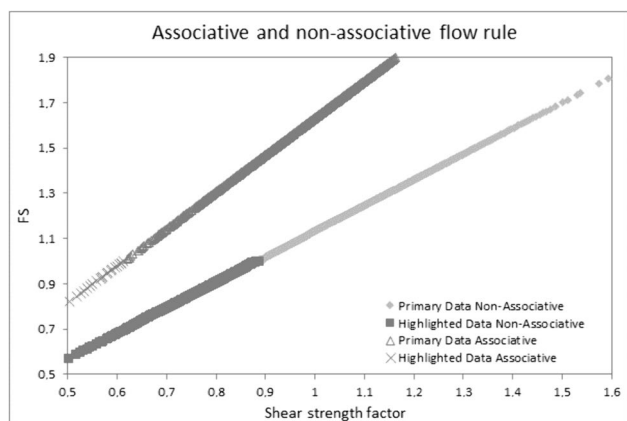**Fig. 11** Distribution of FS values for **a** associative and **b** non-associative flow rule with $\psi = 0°$

Fig. 12 Shear strength factor vs FS for associative and non-associative flow rule with $\psi = 0°$

Fig. 13 Shear/normal function of HB criterion by Serrano et al. (2000) for the analysed case study

Probabilistic analysis

P_f was determined for the associative and the non-associative flow rule of the shear/normal functions defined by Eqs. (6) and (7) (Table 5). For both scenarios, 1000 analyses (sampling iterations) were performed. The convergence plot of the P_f, as shown in Fig. 10a, indicates that convergence in the case of associative flow rule is achieved after approx. 600 iterations. The second scenario (non-associative flow rule) reached a constant value of $P_f = 28.14\%$ after approx. 400 iterations (Fig. 10b). It is interesting to note that the P_f, in the case of the non-associative flow rule, decreases abruptly to the minimum value after less than 50 iterations, while in the case of the associative flow rule P_f steadily increases towards the maximum value (of more than 4%) and then, after sufficient number of iterations reduces to the constant value of 2.70%.

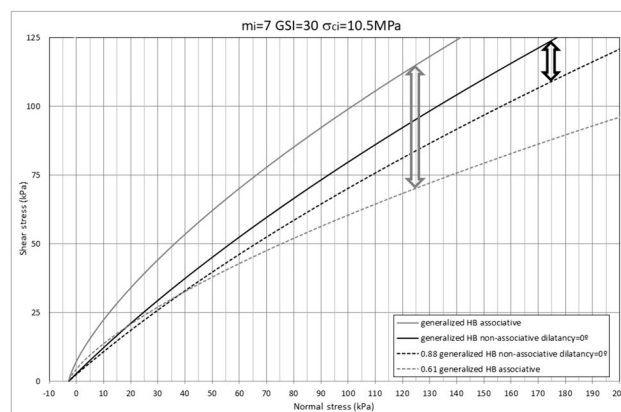Figure 11 shows the distribution of FS values for the two cases analysed (failure criterion introduced by the shear/normal function defined by Eqs. (6) and (7) with the associative and the non-associative flow rule as given in Table 5). A statistical distribution that best fits the FS data is a normal distribution. Highlighted green bars indicate FS values less than 1.0. It is obvious that for the non-associative scenario P_f is much higher and unacceptable for conventional geotechnical practice ($0.1\% < P_f < 3\%$ or $2 < RI < 3$) (US Army Corps of Engineers 1997).

Figure 12 shows the relation between the shear strength factor (being defined as the factor for which the FS of each trial has to be multiplied to obtain FS = 1.0) and the factor of safety (FS). Dark grey dots indicate analyses with FS < 1.0, while light grey dots indicate analyses with FS > 1.0. In the case of the associative flow rule, the shear strength factor for the failure surface with the lowest FS value, after probabilistic analysis, is equal to 0.61, while in the case of the non-associative flow rule strength factor equals 0.88.

Analysis of shear/normal function of HB criterion

Figure 13 summarizes the shear/normal functions of the generalized HB criterion in the form presented by Serrano
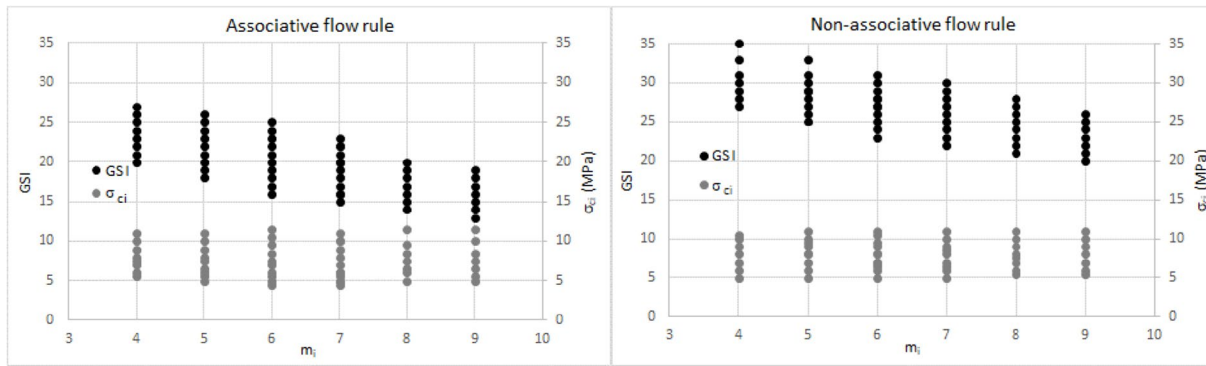
Fig. 14 Correlation between m_i, σ_{ci}, and GSI for the slope failure (FS = 1.0) of the case study for **a** associative and **b** non-associative flow rule with $\psi = 0°$

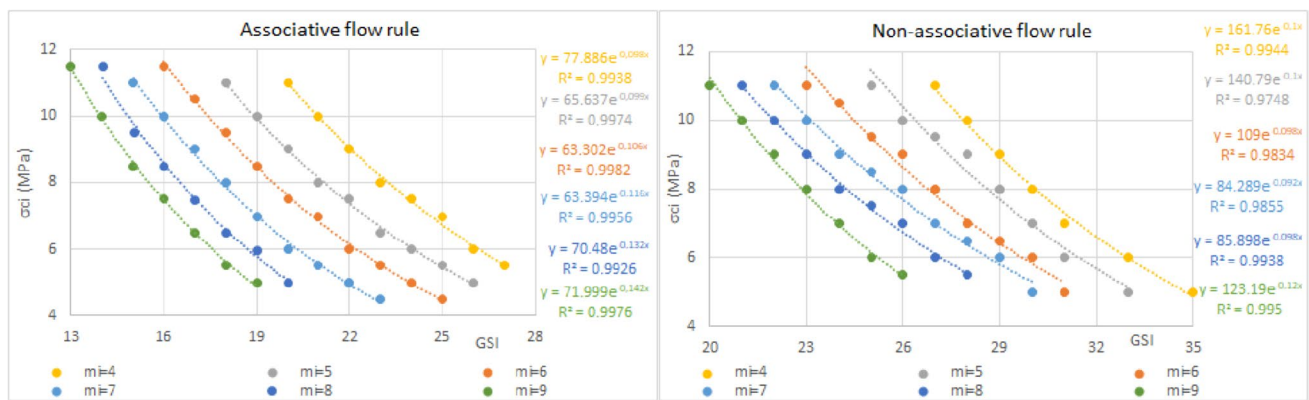**Fig. 15** Relationship between m_i, σ_{ci}, and GSI for FS = 1.0 of the case study for **a** associative and **b** non-associative flow rule with $\psi = 0°$

Table 1 Summary of geometrical and geotechnical parameters necessary for slope stability analysis

Parameter	Case study
Height (m)	12
Slope angle (δ)	45°
Specific unit weight (γ)	25 kN/m^3
GSI	30
Dilatancy angle (ψ)	0°
m_i	7
σ_{ci} (MPa)	10.5
D	0.7
m_b (Eq. 2)	0.1495
s (Eq. 3)	0.000039
a (Eq. 4)	0.5223
$\beta = m_b \cdot \sigma_{ci}/8$ (MPa)	0.1963
$\zeta = 8 \cdot s/m_b^2$	0.01405
k (Eq. 13)	0.9144
A_a (Eq. 13)	0.0131
β_a (MPa) (Eq. 11)	0.1373
ζ_a (Eq. 12)	0.02009

Table 2 Necessary slope angle (δ) for the limit stability FS = 1.0 for the case study

Parameter	Case study	
Dimensionless height $H^* = H/(\beta/\gamma)$	1.53	
Flow type	Associative	Non-associative with $\psi = 0°$
Slope angle (δ) for $\zeta = 0.01$ (Fig. 5)	71°	48°
Slope angle (δ) for $\zeta = 0.1$ (Fig. 5)	85°	68°
Slope angle (δ) ($\zeta = 0.01405$)	72°	49°

et al. (2000) for associative and non-associative flow rule (with $\psi = 0°$). The correlating curves are presented for the set of initially adopted parameters, as summarized in Table 1 (GSI = 30, $\sigma_{ci} = 10.5$ MPa, and $m_i = 7$). Figure 13 also shows the failure criteria range both for associative and non-associative flow rule that leads to rock slope failure (FS = 1.0) according to probabilistic analysis whose summary is given

Table 3 Summary of results of FS for analysed case study under different assumptions for equivalent c′ and φ′

Parameter—case considered/author	Hoek et al. (2002) (Eq. 19)	Li et al. (2008) (δ < 45°) (Eq. 22)	Li et al. (2008) (δ ≥ 45°) (Eq. 21)	Rafiei Renani and Martin (2020) (Eq. 23)
$\sigma_{3max}\prime$ (kPa)	224	110.8	58.1	52.5
φ′ (°) (Eq. 15)	29.03	34.60	39.72	40.51
c′ (kPa) (Eq. 16)	40.05	25.79	17.71	16.75
FS (LEM)	1.78	1.65	1.62	1.62
Error (%)	12.72	4.18	2.47	2.53
FS (FEM) non-associative ψ = 0°	1.72	1.61	1.58	1.58
Error (%)	8.86	1.90	-	0
FS (FEM) associative ψ = φ	1.73	1.62	1.60	1.61
Error (%)	9.50	2.53	1.27	1.90

Table 4 Summary of values of H_L and H_U

Author	Hoek et al. (2002) (Eq. 19)	Li et al. (2008) (δ < 45°) (Eq. 22)	Li et al. (2008) (δ ≥ 45°) (Eq. 21)	Rafiei Renani and Martin (2020) (Eq. 23)
$\sigma_{3max}\prime$ (kPa)	224	110.8	58.1	52.5
H_L (m)	5.44	3.93	3.01	2.91
H_U (m)	10.88	7.85	6.04	5.81

in Fig. 12 (estimated as 0.61 for associative and 0.88 for non-associative flow rule with ψ = 0°).

Figure 14 shows the relationship between different HB parameters (m_i, σ_{ci}, and GSI) that would produce the failure under certain combinations. Input parameters were varied until they produced the shear strength envelope reasonably well matched to the weighted failure envelope (for associative and non-associative flow rule, represented as dotted lines in Fig. 13). For example, it can be observed that for the same m_i value, the corresponding range of σ_{ci} and GSI values is almost the same for different flow rules; however, the higher GSI value to obtain FS = 1.0 is necessary in the case of the non-associative flow rule.

Figure 15 presents the relationship between σ_{ci} and GSI for different m_i values for limit state condition FS = 1, shown both for associative and non-associative flow rule. If the combination of these parameters is introduced into shear/normal function, it would lead to failure of the rock slope.

Several important assumptions and conclusions can be derived from previous considerations:

(i) The associative flow rule overestimates the rock mass strength, overestimating FS of the rock slope, in comparison to the non-associative flow rule.

(ii) For the analysed slope case study to reach the state of failure, the shear/normal function should be factored by 0.88 and 0.61, for the case of non-associative and associative flow rules, respectively (Fig. 13).

(iii) The variability of GSI and σ_{ci} in relation to m_i value (for the weighted failure criteria that leads to slope failure) is presented in Fig. 14. It can be observed that with an increase of m_i, the range of σ_{ci} values practically remains unchanged, while the variation of GSI is more pronounced. It can be observed that for the same combination of m_i and σ_{ci}, values of

Table 5 Summary of FS under different assumptions for the case study applying shear/normal function

Method	Shear/normal function (Eqs. 6 and 7) associative ψ = 0		Shear/normal function (Eqs. 6 and 7) non-associative ψ = 0°		Generalized HB (2002)		
	LEM	FEM	LEM	FEM	LEM	FEM associative $m_{dil} = m_b$	FEM non-associative $m_{dil} = 0$
FS	1.637	1.64	1.138	1.12	1.648	1.64	1.61
Error (%)	46	46	1.6	-	47	46	43

Table 6 CoV of parameters GSI, m_i, and σ_{ci} for different flow rules

	Associative $\psi = 0$	Non-associative with $\psi = 0°$	Rafiei Renani and Cai 2022)
GSI	0.176	0.125	0.1–0.2
m_i	0.277	0.280	0.1–0.3
σ_{ci}	0.284	0.232	0.1–0.5

GSI are lower for the associative flow rule. With an increasing value of m_i and corresponding range of σ_{ci}, the value of GSI decreases.

(iv) It is possible to determine the combination of GSI and σ_{ci} values for constant m_i, necessary to reach the rock slope failure for associative and non-associative scenario, as summarized in Fig. 15.

(v) The charts presented in Fig. 15 are valid for considered case study and could be used for the quick estimation of the combination of input parameters that would lead to rock slope failure taking into account the extent of uncertainty in defining initial values of input parameters GSI, m_i, and σ_{ci}.

(vi) The shear/normal function is dependent on the initially estimated geotechnical parameters GSI, m_i, and σ_{ci}. The variability of values of these influencing parameters on the failure criterion (Fig. 15) can be defined by the coefficient of variation (CoV). Table 6 summarizes the CoV for associative and non-associative flow rule with $\psi = 0°$ that leads to failure, observing that CoV is greater for GSI and σ_{ci} parameters for associative than that of the non-associative flow rule, being negligible the difference for m_i. Nevertheless, these CoV values are in accordance with the values summarized in Rafiei Renani and Cai (2022).

Conclusions

Based on the analysis and results given in this study, the following conclusions can be derived:

(i) The alternative application of the generalized HB failure criterion by the shear/normal function (valid both for the associative and non-associative flow rule) and its simple incorporation into commercial codes for slope stability analysis is presented. This shear/normal stress failure criterion is independent of the estimated $\sigma_{3max}\prime$ value omitting the need for calculating equivalent MC parameters.

(ii) If the associative flow rule is applied through the shear/normal function for the generalized HB failure criterion, both in LEM and FEM, the FS value is overestimated compared to the non-associative flow rule. This is in agreement with the findings of Melentijevic (2005) and Melentijevic et al. (2017).

(iii) The comparison between the failure patterns obtained by LEM and FEM shows that the corresponding failed area from LEM is smaller compared to the one obtained by FEM. Also, the different assumption on the flow rule influences the position of the failure surface within the slope. The hypothesis of the non-associative flow rule produces shallower failure surfaces.

(iv) Careful choice of $\sigma_{3max}\prime$ value for the estimation of equivalent MC parameters is of prime importance for proper slope stability analysis. The limitation of stress-dependent linear Mohr–Coulomb parameters is emphasized by analysing the vertical cut problem, for which, depending on the chosen stress level, different critical heights are obtained for the same material.

(v) The best estimation of the maximum minor principal stress level $\sigma_{3max}\prime$ should be related to the thickness of the failed material.

(vi) A cautious estimate of initial input geotechnical parameters (GSI, m_i, σ_{ci}) for HB failure criterion should be done. It is necessary to define the range of input parameters instead of unique value in order to take into account the variability of the possible subjective choice of in situ rock mass properties. In this sense, probabilistic analysis should be performed to properly consider possible variability of rock mass properties estimated in situ.

(vii) If slope stability analysis for the considered case study is performed with an assumption of associative flow rule, the P_f is less than 3% which is considered acceptable. If the non-associative flow rule is employed, the probability of failure is rather high with $P_f = 27.8\%$, whereas the deterministic safety factor value is close to 1. This is in accordance with the field observations.

(viii) Charts are developed for the analysed case study for quick initial estimation of rock mass parameters σ_{ci}, GSI, and m_i, both for associative and non-associative flow rule that would lead to slope failure. Similar charts should be developed for each case study to reduce the subjective engineering choice on the value of GSI since σ_{ci} and m_i could be more reliably determined by means of laboratory tests.

(ix) With the same values of m_i and σ_{ci}, the higher GSI values lead to failure under the hypothesis of the non-associative flow rule compared to the associative one.

(x) The necessary incorporation of non-associative flow rule into slope stability analysis is emphasized.

Declarations We hereby declare that this work entitled: "Rock slope stability analysis under Hoek–Brown failure criterion with different flow rules" submitted to the *Bulletin of Engineering Geology and the Environment* is a record of original work done by the authors. The information and data given in the study are authentic. This material is not submitted to any other publisher.

Conflict of interest The authors declare no competing interests.

References

Alejano L, Alonso E (2005) Considerations of the dilatancy angle in rocks and rock masses. Int J Rock Mech Min Sci 42:481–507. https://doi.org/10.1016/j.ijrmms.2005.01.003

Alencar A, Melentijevic S, Galindo R (2019) The influence of the dilatancy on the ultimate bearing capacity of the rock mass. In Proc. XVII ECSMGE–2019. https://doi.org/10.32075/17ECSMGE-2019-0447

Alencar A, Galindo R, Olalla C, Melentijevic C (2021) Bearing capacity of footings on rock masses using flow laws. Appl Sci 2021(11):11829. https://doi.org/10.3390/app112411829

Benz T, Schwab R, Kauther RA, Vermeer PA (2008) A Hoek-Brown criterion with intrinsic material strength factorization. Int J Rock Mech Min Sci 45(2):210–222

Berisavljevic Z, Berisavljevic D, Rakic D, Radic Z (2018) Application of geological strength index for characterization of weathering-induced failures. Gradjevinar 70(10):891–903. https://doi.org/10.14256/JCE.1876.2016

Carranza-Torres C (2004) Some comments on the application of the Hoek-Brown failure criterion for intact rock and rock masses to the solution of tunnel and slope problems. In: Barla G, Barla M (eds) Proc MIR 2004–X Conference on Rock and Engineering Mechanics, vol 24–25. Torino, pp 285–326

Cheng YM, Lansivaara T, Wei WB (2007) Two-dimensional slope stability analysis by limit equilibrium and strength reduction methods. Comp Geotech 34:137–150. https://doi.org/10.1016/j.compgeo.2006.10.011

Davis RO, Selvadurai APS (2002) Plasticity and geomechanics. Cambridge University Press, Cambridge, p 287

El-Ramly H, Morgenstern NR, Cruden DM (2002) Probabilistic slope stability analysis for practice. Can Geotech J 39:665–683

EN 1997–1: 2004. Eurocode 7: Geotechnical design - Part 1: General rules

García Wolfrum S (2005) Anclajes en roca. PhD Thesis Universidad Politécnica de Madrid, Spain

Griffiths DV, Lane PA (1999) Slope stability analysis by finite elements. Geotechnique 49(3):378–403

Griffiths DV, Fenton GA (2004) Probabilistic slope stability analysis by finite elements. ASCE J Geotech Geoenviron Eng 130:507–518. https://doi.org/10.1061/(ASCE)1090-0241(2004)130:5(507)

Guo X, Sun Q, Dias D, Antoinet E (2020) Probabilistic assessment of an earth dam stability design using the adaptive polynomial chaos expansion. Bull Eng Geol Environ 79:4639–4655. https://doi.org/10.1007/s10064-020-01847-2

Hammah R, Jacoub T, Corkum B, Curran J (2005) A comparison of finite element slope stability analysis with conventional limit equilibrium investigations, Proc 58th Canadian Geotechnical and 6th Joint IAH-CNC and CGS Groundwater Specialty Conferences

Hoek E, Brown ET (1980) Empirical strength criterion for rock masses. J Geotech Engng Div ASCE 106:1013–1035

Hoek E, Bray JW (1981) Rock slope engineering, 3rd edn. Instn. Min. Metall, London

Hoek E, Wood D, Shah S (1992) A modified Hoek-Brown criterion for jointed rock masses. In: Hudson JA (ed) Proc Symposium ISRM: rock Characterization (Eurock 92). British Geotechnical Society, London, pp 209–214

Hoek E, Brown ET (1997) Practical estimates of rock mass strength. Int J Rock Mech Min Sci 34(8):1165–1186

Hoek E, Brown ET (2019) The Hoek-Brown failure criterion and GSI-2018 edition. J Rock Mech Geotech Eng. https://doi.org/10.1016/j.jrmge.2018.08.001

Hoek E, Carranza-Torres C, Corkum B (2002) Hoek-Brown failure criterion-2002 edition. In: Proc North Symposium, Toronto, pp 718–742

Iman RL, Davenport JM, Zeigler DK (1980) Latin hypercube sampling (program user's guide)

Javankhoshdel S, Bathurst RJ (2016) Influence of cross-correlation between soil parameters on probability of failure of simple cohesive and c-φ slopes. Can Geotech J 53(5):839–853

Javankhoshdel S, Luo N, Bathurst RJ (2017) Probabilistic analysis of simple slopes with cohesive soil strength using RLEM and RFEM. Georisk 11(3):231–246

Jiménez R, Serrano A, Olalla C (2008) Linearization of the Hoek and Brown rock failure criterion for tunnelling in elasto-plastic rock masses. Int J Rock Mech Min Sci 45:1153–1163

Johari A, Hajivand AK, Binesh S (2020) System reliability analysis of soil nail wall using random finite element method. Bull Eng Geol Environ 79:2777–2798. https://doi.org/10.1007/s10064-020-01740-y

Kumar V, Burman A, Himanshu N, Gordan B (2021) Rock slope stability charts based on limit equilibrium method incorporating Generalized Hoek-Brown strength criterion for static and seismic conditions. Environ Earth Sci 80:212. https://doi.org/10.1007/s12665-021-09498-6

Li AJ, Merifield RS, Lyamin AV (2008) Stability charts for rock slopes based on the Hoek-Brown failure criterion. Int J Rock Mech Min Sci 45:689–700

Li AJ, Lyamin AV, Merifield RS (2009) Seismic rock slope stability charts based on limit analysis methods. Comp Geotech 36:135–148

Li AJ, Merifield RS, Lyamin AV (2011) Effect of rock mass disturbance on the stability of rock slopes using the Hoek-Brown failure criterion. Comp Geotech 38(4):546–558

Ma T, Cami B, Javankhoshdel S, Yacoub T, Corkum B, Curran J (2022) Effect of disturbance factor distribution function on

stability of an open pit mine. In: Proc American Rock Mech Assoc pp 718–742

Manzanas J (2002) Estabilidad de taludes rocosos infinitos con criterios de rotura no lineales y leyes de fluencia no asociada. PhD Thesis Universidad Politécnica de Madrid, Spain

McKay MD, Beckman RJ, Conover WJ (1979) A comparison of three methods for selecting values of input variables in the analysis of output from a computer code. Technometrics 21(2):239–245

Melentijevic S (2005) Estabilidad de taludes en macizos rocosos con criterios de rotura no lineales y leyes de fluencia no asociada. PhD Thesis Universidad Politécnica de Madrid, Spain

Melentijevic S, Serrano A, Olalla C (2005) Cálculo de taludes en medios rocosos con deslizamiento plano y deslizamiento circular con el criterio de rotura de Hoek & Brown. In: Dulcet JCI, Alonso E, Ruiz MR, Ziegler MH (eds) Proc VI Simposio Nacional sobre Taludes y Laderas Inestables, vol 2. pp 985–996

Melentijevic S, Serrano A, Olalla C (2006) Planar slope stability analysis of soft and highly fractured rock masses with the Hoek & Brown failure criterion and non-associative plasticity flow rule. In: Logar J, Gaberc A, Majes B (eds) Proc XIII Danube - European Conference on Geotechnical Engineering, Slovenian geotechnical society, pp 651–656

Melentijevic S, Serrano A, Olalla C, Galindo RA (2017) Incorporation of non-associative flow rules into rock slope stability analysis. Int J Rock Mech Min Sci 96:47–57. https://doi.org/10.1016/j.ijrmms2017.04.010

Morgenstern NR, Price VE (1965) The analysis of the stability of general slip surfaces. Geotechnique 15:79–93

Naznin R (2007) Equivalent Mohr-Coulomb dilation parameter for Hoek-Brown rock. In: MSc thesis. Laurentian University, Ontario, Canada, p 192

Rafiei Renani H, Martin CD, Varona P, Lorig L (2019) Stability analysis of slopes with spatially variable strength properties. Rock Mech Rock Eng 52:3791–3808. https://doi.org/10.1007/s00603-019-01828-2

Rafiei Renani H, Cai M (2022) Forty-year review of the Hoek-Brown failure criterion for jointed rock masses. Rock Mech Rock Eng 55(4):1–23. https://doi.org/10.1007/s00603-021-02661-2

Rafiei Renani H, Martin CD (2020) Slope stability analysis using equivalent Mohr-Coulomb and Hoek-Brown criteria. Rock Mech Rock Eng 53:13–21. https://doi.org/10.1007/s00603-019-01889-3

Reig I (2004) Estudio de la convergencia de túneles circulares en macizos elastoplásticos con criterios de resistencia no lineales y leyes de fluencia no asociadas. PhD Thesis Universidad Politécnica de Madrid, Spain

Robert C, Casella G (2004) Monte Carlo statistical methods. Springer-Verlag. https://doi.org/10.1007/978-1-4757-4145-2

Rocscience Inc. (2022a) SLIDE- 2D limit equilibrium analysis of slope stability, version 9.020. Toronto

Rocscience Inc. (2022b) RS2- 2D finite element analysis of geotechnical structures, version 11.013. Toronto

Rose ND, Scholz M, Burden J, King M, Maggs C, Havaej M (2018) Quantifying transitional rock mass disturbance in open pit slopes related to mining excavation. In: Proc XIV Congreso Internacional de Energia y Recursos Minerales, Seville, Spain

Serrano A, Castillo Ron E (1973) Análisis probabilista de la estabilidad de taludes rocosos. Boletín de Información del Laboratorio del Transporte y Mecánica del Suelo. CEDEX. MOPU nº 100 (9–20)

Serrano A, Olalla C (1994) Ultimate bearing capacity of rock masses. Int J Rock Mech Min Sci 31(2):93–106

Serrano A, Olalla C, Gonzalez J (2000) Ultimate bearing capacity of rock masses based on the modified Hoek-Brown criterion. Int J Rock Mech Min Sci 37(6):1013–1018. https://doi.org/10.1016/S1365-1609(00)00028-9

Serrano A, Olalla C, Perucho A (2002) Planar failure surfaces on rock assuming a non-linear strength law and constant dilatancy. In: Gama D, Ribeiro e Sousa L (eds) Proc Int Symp on Rock Engineering for Mountainous Regions, EuRock 2002, ISRM, Funchal, pp 179–186

Serrano A, Olalla C (2004) Closed form solution of planar rock slope stability under Hoek and Brown (1980) failure criterion and non-associative plasticity. In: Lacerda WA (ed) Proc of Landslides: evaluation and stabilization, Rotterdam: Balkema, Rio de Janeiro, pp 533–537

Serrano A, Olalla C, Manzanas J (2005) Stability of highly fractured infinite rock slopes with nonlinear failure criteria and non-associated flow laws. Can Geotech J 42:393–411

Serrano A, Olalla C, Reig I (2011) Convergence of circular tunnels in elastoplastic rock masses with non-linear failure criteria and non-associated flow laws. Int J Rock Mech Min Sci 48:878–887. https://doi.org/10.1016/j.ijrmms.2011.06.008

Shen J, Karakus M, Xu C (2013) Chart-based slope stability assessment using the generalized Hoek-Brown criterion. Int J Rock Mech Min Sci 64:210–219

Silva-Guzmán R, Gómez P (2015) Towards a mechanically based definition of the disturbance factor using the "slope model" lattice code. In: Proc ISRM Regional Symposium – 8th South American Congress on Rock Mechanics, Buenos Aires, Argentina

Sofianos AI (2003) Tunnelling Mohr-Coulomb strength parameters for rock masses satisfying the generalized Hoek-Brown criterion. Int J Rock Mech Min Sci 40:435–440. https://doi.org/10.1016/S1365-1609(03)00017-0

Sofianos AI, PP, Nomikos (2006) Equivalent Mohr-Coulomb and generalized Hoek-Brown strength parameters for supported axisymmetric tunnels in plastic or brittle rock. Int J Rock Mech Min Sci 43:683–704. https://doi.org/10.1016/j.ijrmms.2005.11.006

Taylor DW (1937) Stability of earth slopes. J Boston Soc Civil Eng XXIV 3:337–386

Tietje O, Fitze P, Schneider HR (2014) Slope stability analysis based on autocorrelated shear strength parameters. Geotech Geol Eng 32:1477–1483. https://doi.org/10.1007/s10706-013-9693-8

US Army Corps of Engineers (1997) Engineering and design: introduction to probability and reliability methods for use in geotechnical engineering Technical Letter No. 1110–2–547, Washington DC

Wang L, Wu C, Gu X, Liu H, Mei G, Zhang W (2020) Probabilistic stability analysis of earth dam slope under transient seepage using multivariate adaptive regression splines. Bull Eng Geol Environ 79:2763–2775. https://doi.org/10.1007/s10064-020-01730-0

Wei Y, Fu W, Ye F (2018) Estimation of the equivalent Mohr-Coulomb parameters using the Hoek-Brown criterion and its application in slope analysis. Eur J Environ Civ Eng. https://doi.org/10.1080/19648189.2018.1538904

Yang XL, Yin JH (2010) Slope equivalent Mohr-Coulomb strength parameters for rock masses satisfying the Hoek-Brown criterion. Rock Mech Rock Eng 43:505–511. https://doi.org/10.1007/s00603-009-0044-2

Zhang J, Tang WH, Zhang LM (2010) Efficient probabilistic back-analysis of slope stability model parameters. J Geotech Geoenvir Eng 136(1):99–109. https://doi.org/10.1061/(ASCE)GT.1943-5606.0000205

Zhou X, Chen J, Chen Y, Song S, Shi M, Zhan J (2017) Bayesian-based probabilistic kinematic analysis of discontinuity-controlled rock slope instabilities. Bull Eng Geol Environ 76:1249–1262. https://doi.org/10.1007/s10064-016-0972-5

Zuo J, Shen J (2020) The Hoek-Brown failure criterion – from theory to application. Ed Springer. https://doi.org/10.1007/978-981-15-1769-3